Journal of Sound and Vibration (1998) **213**(1), 139–158

COMPUTING CRITICAL SPEEDS FOR ROTATING MACHINES WITH SPEED DEPENDENT BEARING PROPERTIES

M. I. Friswell

Department of Mechanical Engineering, University of Wales Swansea, Swansea SA2 8PP, Wales

S. D. Garvey and J. E. T. Penny

Dynamics, Control and Vibration Research Group, Department of Mechanical and Electrical Engineering, Aston University, Birmingham B4 7ET, England

AND

M. G. Smart

Department of Mechanical Engineering, University of Wales Swansea, Swansea SA2 8PP, Wales

(*Received* 26 *August* 1997, *and in final form* 6 *January* 1998)

In this paper available methods are examined for computing critical speeds for rotating machines whose bearings have speed dependent properties and a modification is proposed which can be incorporated into almost all of the established techniques. The established methods for the calculation of critical speeds are adequately efficient when only a single configuration is analyzed. The trend towards incorporating critical speed calculations into the design optimization process and model-based fault diagnosis systems requires the more efficient calculation of critical speeds. The proposed modification involves replacing the sets of speed-dependent bearing characteristics by fictitious multi-degree-of-freedom systems whose characteristics emulate those of the bearings themselves. The method by which these fictitious systems can be found is explained and the advantages of using this method for computing critical speeds are demonstrated in conjunction with the finite element approach to evaluating critical speeds. The proposed technique is also well suited to computing efficiently the machine response to unbalance by using a truncated modal decomposition.

1. INTRODUCTION

In the design of large rotating machinery, one of the most fundamental considerations is the set of values of the critical speeds relative to the intended operating speed range of the machine. Before the availability of reliable calculation procedures and computational hardware on which to execute them, there was a strong tendency to design "rigid-rotor" machines which would have no critical speeds below the highest speed of interest in the operating range. In the design of steam turbines in particular, this tendency imposed severe limitations on the maximum size of plant. With the arrival of multi-element models of rotor/stator systems and powerful computers, machine designers are now confidently designing machines to have several critical speeds below the maximum operating speed.

0022–460X/98/210139 + 20 $25.00/0/sv981503

Computationally, finding critical speeds is not straightforward, particularly for machines having journal bearings because the dynamic properties of these bearings are strongly dependent on rotor speed. There are several established solutions of this problem and these are discussed in this paper. Although the power of modern computing hardware is such that computing a set of critical speeds for a single machine design is not usually sufficiently time-consuming to be of any concern, the trend towards building the calculation of critical speeds into a design optimization process [1, 2] combined with the need to examine the many possible combinations of misalignment and various operating conditions of multi-bearing machines, means that these calculations may be required numerous times in the automated search for an optimal machine design. The proposed method may also be used in model-based diagnosis of faults in rotating machines.

In this paper, a technique is proposed which significantly streamlines the calculation of critical speeds for machinery whose bearing characteristics are dependent on shaft speed. This involves setting up fictitious multi-degree-of-freedom systems between the stationary and rotating parts of the bearing to emulate the frequency response function of the journal bearings. Although these degrees of freedom are not physical, the resulting systems can be regarded as reduced order models of the complex bearing dynamics. The calculation of critical speeds is then reduced to a simple eigenvalue solution like that required for the calculation of resonances of a stationary structure and the dimension of this eigenvalue problem is only slightly greater than the dimension of the eigenvalue problem which would have to be solved to establish critical speeds if the bearing properties were independent of speed. One very attractive aspect of this technique is that any program which can perform dynamic calculations for a rotor–stator system given a fixed set of bearing characteristics can be used without modification to compute the true critical speeds of a system in which the bearing characteristics vary significantly with speed.

The proposed technique is also well suited to efficiently computing the machine response to unbalance using a truncated modal decomposition. The current approach for machines with speed dependent bearings requires the response to be calculated from the dynamic stiffness matrix at every rotor speed. In many machines, where only a few of the system modes are excited, the modal decomposition approach would require far less computation. This method is not considered further, since it is a straightforward extension of the critical speed calculations once the system matrices have been set up.

The actual dependence of bearing characteristics on speed is a matter of some tribological complexity and continues to be the subject of intense study. It is well established, however, that the dynamic stiffness properties of any hydrodynamic bearing for small oscillations at synchronous frequency can be represented by using one 2×2 stiffness matrix (over the field of real numbers) and one 2×2 viscous damping matrix (also over the field of real numbers) if the bearing is sufficiently short. A longer bearing might require two 4×4 matrices to account for the effects of angular oscillations of the shaft with respect to the bearing about a diametral axis. The method of this paper is described in terms of short bearings but is no less applicable to the longer bearings case.

It will be assumed for the purposes of this paper that empirical relationships have already been derived for the stiffness and damping matrices of any bearing which might be considered for inclusion into a machine design and that these relationships are smooth.

2. ANALYSIS METHODS FOR EVALUATING CRITICAL SPEEDS

The existing methods for computing critical speeds for rotating machinery can be categorised as pure finite element models, numerical transfer matrix models, and analytical transfer matrix models (or hybrid models including finite elements).

It would appear from the literature that in the majority of current computer programs for rotor dynamics calculations the transfer matrix concept is used. The concept of the transfer matrix method is well established and understood, having been originated by Myklestadt [3] in 1944 for static beams and subsequently developed by Prohl [4] for rotors. Employing the transfer matrix technique in some form has much to recommend it as evidenced by the proportion of the researchers who advocate the use of a transfer matrix model for the rotor [5–11]. The strongest advantage in using a transfer matrix representation for the rotor is that it is not necessary to create very large system matrices to represent the rotating part of the system.

Finite element methods enable general purpose programs to be written for computing critical speeds [12–17]. Pure finite element methods for computing critical speeds do require substantially more computer memory than their transfer matrix counterparts and this disadvantage has been a powerful argument if favour of transfer matrix or hybrid methods. However, with current computer hardware, there are very few rotating machines that cannot be modelled with more numerical accuracy than necessary, in more detail than necessary and for a greater range of frequencies than is necessary by using a finite element model. If this model is set up by an experienced rotor-dynamicist, it is almost certain that any significant discrepancy between the predictions based on the model and measurements made on the physical machine would have a lot more to do with errors in the model parameters than with a lack of detail in the model.

An exhaustive comparison of the respective merits of finite element and transfer matrix methods is beyond the scope of this paper. For example, it is arguable whether the computational time taken by finite element methods is greater than or less than that required for a transfer matrix approach in general. The authors observe that the trend in the literature is towards full finite element models. The recent text by Lalanne and Ferraris [16], for example, does not include any mention of transfer matrix methods. The text by Childs [17] devotes very little attention to the problem of computing critical speeds for the general rotating machine but one chapter is devoted largely to developing a system model and the bulk of this focuses on finite element type models. Childs does note the considerable computation required for the repeatedly manipulation of the large matrices which automatically result from many real analyses and pays particular attention to methods by which the size of the matrices can be dramatically reduced.

In the present paper it is proposed that a fictitious dynamic system can be incorporated between the shaft and the bearing support system in any model for a rotating machine as a means of approximating the speed dependence of the bearing characteristics, rather than using speed dependent stiffness and damping matrices. This concept provides no advantage in numerical transfer matrix methods because the combined bearing and support properties are computed numerically for each individual speed. It does, however, provide a considerable advantage in finite element and analytical transfer matrix methods. The method is presented in the context of pure finite element models.

3. EVALUATING CRITICAL SPEEDS USING FINITE ELEMENT MODELS

Suppose that a finite element model has been created to represent all aspects of a particular rotating machine except the bearing characteristics. Implicitly, therefore, the rotor and stator of the machine are completely uncoupled. Given that they must eventually be coupled together to analyze the complete machine, it is sensible to model the rotor and stator using a single reference frame and the usual choice is the stationary frame.

It is normal practice in dynamic analysis with finite element models to perform static (Guyan) reduction to reduce the number of active degrees of freedom in the model before either solving for natural frequencies or computing either transient or steady state response and one can suppose that this reduction or *condensation* has taken place for both the stator and the rotor such that for the range of frequency of interest with the model and the accuracy desired, all of the remaining degrees of freedom are deemed to be "necessary". Note that certain degrees of freedom at the bearing locations on both the rotor and the stator must be retained through the condensation process to allow for the rotor and stator to be coupled subsequently.

The condensed vector of displacement co-ordinates $\mathbf{u}$ will be used to represent the set of harmonic displacements (at angular frequency ω rad/s). Assume that the full model of the rotor/bearing/foundation system may be partitioned by using degrees of freedom (DoFs) relating to the rotor and the foundation. Both sets of DoFs may be further partitioned into internal DoFs and DoFs at the bearings. It is assumed that the bearings can be modelled by using DoFs on the rotor and on the foundation only, so that the bearing model does not contain any internal DoFs. Thus the equations of motion of the system, in terms of dynamic stiffness matrices, may be written as

$$\text{for the rotor,} \quad \begin{bmatrix} \mathbf{D}_{R,II} & \mathbf{D}_{R,IB} \\ \mathbf{D}_{R,BI} & \mathbf{D}_{R,BB} \end{bmatrix} \begin{Bmatrix} \mathbf{u}_{R,I} \\ \mathbf{u}_{R,B} \end{Bmatrix} = \begin{Bmatrix} \mathbf{f}_{R,I} \\ -\mathbf{f}_{F,B} \end{Bmatrix}, \tag{1}$$

$$\text{for the bearings,} \quad \begin{bmatrix} \mathbf{B} & -\mathbf{B} \\ -\mathbf{B} & \mathbf{B} \end{bmatrix} \begin{Bmatrix} \mathbf{u}_{R,B} \\ \mathbf{u}_{F,B} \end{Bmatrix} = \begin{Bmatrix} \mathbf{f}_{F,B} \\ -\mathbf{f}_{F,B} \end{Bmatrix}, \tag{2}$$

$$\text{for the foundation,} \quad \begin{bmatrix} \mathbf{D}_{F,BB} & \mathbf{D}_{F,BI} \\ \mathbf{D}_{F,IB} & \mathbf{D}_{F,II} \end{bmatrix} \begin{Bmatrix} \mathbf{u}_{F,B} \\ \mathbf{u}_{F,I} \end{Bmatrix} = \begin{Bmatrix} \mathbf{f}_{F,B} \\ \mathbf{0} \end{Bmatrix}. \tag{3}$$

In equations (1)–(3), $\mathbf{D}$ represents a dynamic stiffness, $\mathbf{u}$ the response, and $\mathbf{f}$ a force. The first subscript, R and F, represents the rotor and foundation models. The second subscripts represent the DoFs at the bearing (B) or at internal DoFs (I). The force $\mathbf{f}_{R,I}$ represents the force on the internal rotor DoFs and includes the out-of-balance forces. It is assumed that no external force is applied to the foundation.

Note that the special form of the bearing dynamic stiffness matrix arises from the assumption that the force required to produce a given relative bearing deflection depends only on the relative displacement, $\mathbf{u}_{R,B} - \mathbf{u}_{F,B}$, and this force acts equally and oppositely on the rotor and on the foundation. The only force into the foundations is assumed to be from the bearings. Any force excitation applied to the foundations will produce extra force terms in equation (3).

Equations (1)–(3) may be combined to give the full equations of motion:

$$\begin{bmatrix} \mathbf{D}_{R,II} & \mathbf{D}_{R,IB} & \mathbf{0} & \mathbf{0} \\ \mathbf{D}_{R,BI} & \mathbf{D}_{R,BB} + \mathbf{B} & -\mathbf{B} & \mathbf{0} \\ \mathbf{0} & -\mathbf{B} & \mathbf{B} + \mathbf{D}_{F,BB} & \mathbf{D}_{F,BI} \\ \mathbf{0} & \mathbf{0} & \mathbf{D}_{F,IB} & \mathbf{D}_{F,II} \end{bmatrix} \begin{Bmatrix} \mathbf{u}_{R,I} \\ \mathbf{u}_{R,B} \\ \mathbf{u}_{F,B} \\ \mathbf{u}_{F,I} \end{Bmatrix} = \begin{bmatrix} \mathbf{f}_{R,I} \\ \mathbf{0} \\ \mathbf{0} \\ \mathbf{0} \end{bmatrix}. \tag{4}$$

The dynamic stiffness matrices may be written in terms of the mass, damping, gyroscopic and stiffness matrices of the rotor, $\mathbf{M}_R$, $\mathbf{C}_R$, $\mathbf{G}_R$ and $\mathbf{K}_R$, and of the foundation, $\mathbf{M}_F$, $\mathbf{C}_F$ and $\mathbf{K}_F$, where, for example,

$$\mathbf{D}_R = (\mathrm{j}\omega)^2\mathbf{M}_R + \mathrm{j}\omega[\mathbf{C}_R + \Omega\mathbf{G}_R] + \mathbf{K}_R = \begin{bmatrix} \mathbf{D}_{R,II} & \mathbf{D}_{R,IB} \\ \mathbf{D}_{R,BI} & \mathbf{D}_{R,BB} \end{bmatrix}. \tag{5}$$

In general these structural matrices are determined as condensed mass, stiffness, gyroscopic and damping matrices. The mass, damping and stiffness matrices for the rotor and the foundation are generally symmetric. The gyroscopic effects are linear in the rotational speed, Ω, and the gyroscopic matrix, $\mathbf{G}_R$, is skew-symmetric. The bearing dynamic stiffness is usually speed dependent, so that $\mathbf{B} = \mathbf{B}(\Omega)$, and is generally non-symmetric.

For the purposes of this paper, the only source of forcing considered is unbalance forcing whose frequency is equal to the rotor spin speed. Thus $\omega = \Omega$. Equation (4) can be used to form another equation which directly expresses the criterion for a critical speed. There are actually two possible definitions of critical speed. On the one hand Ianuzzelli [18], for example, defined a critical speed as a rotor spin speed at which the response to unbalance forcing (which rises in proportion to Ω^2) reaches a local maximum. Depending on the damping in the system, this "critical speed" can be significantly different from the critical speed defined by the frequency that minimizes

$$\det \begin{bmatrix} \mathbf{D}_{R,II} & \mathbf{D}_{R,IB} & \mathbf{0} & \mathbf{0} \\ \mathbf{D}_{R,BI} & \mathbf{D}_{R,BB} + \mathbf{B} & -\mathbf{B} & \mathbf{0} \\ \mathbf{0} & -\mathbf{B} & \mathbf{B} + \mathbf{D}_{F,BB} & \mathbf{D}_{F,BI} \\ \mathbf{0} & \mathbf{0} & \mathbf{D}_{F,IB} & \mathbf{D}_{F,II} \end{bmatrix}. \tag{6}$$

The two definitions differ most in the cases of critical speeds for which the damping ratio is quite high but for practical purposes, if the damping is relatively high, then the exactness of the predicted critical speed is not important. The "local maximum in unbalance response" definition actually depends to some extent on the position of the unbalance whereas the other definition based on Equation (6) depends only on the system. For the remainder of this paper, the definition used for critical speed, Ω_{crit}, will be based on equation (6).

If the mass, damping and stiffness matrices are independent of Ω, then the critical speeds may be calculated by solving the following eigenvalue problem

$$\left[\begin{bmatrix} \mathbf{0} & \mathbf{K} \\ \mathbf{K} & \mathbf{C} \end{bmatrix} - s\begin{bmatrix} \mathbf{K} & \mathbf{0} \\ \mathbf{0} & -\mathbf{M} \end{bmatrix}\right]\mathbf{v} = \mathbf{0}, \tag{7}$$

where

$$\mathbf{K} = \begin{bmatrix} \mathbf{K}_{R,II} & \mathbf{K}_{R,IB} & \mathbf{0} & \mathbf{0} \\ \mathbf{K}_{R,BI} & \mathbf{K}_{R,BB} + \mathbf{B} & -\mathbf{B} & \mathbf{0} \\ \mathbf{0} & -\mathbf{B} & \mathbf{B} + \mathbf{K}_{F,BB} & \mathbf{K}_{F,BI} \\ \mathbf{0} & \mathbf{0} & \mathbf{D}_{F,IB} & \mathbf{K}_{F,II} \end{bmatrix},$$

$$\mathbf{C} = \begin{bmatrix} \mathbf{C}_R & \mathbf{0} \\ \mathbf{0} & \mathbf{C}_F \end{bmatrix}, \qquad \mathbf{M} = \begin{bmatrix} \mathbf{M}_R & \mathbf{0} \\ \mathbf{0} & \mathbf{M}_F \end{bmatrix}.$$

Here, for clarity, it has been assumed that the gyroscopic effects are negligible. The eigenvalues, s, contain the critical speed as the imaginary part. The corresponding eigenvector determines how the machine behaves close to the critical speed. If gyroscopic effects are not negligible then the gyroscopic matrix will enter in the mass matrix $\mathbf{M}$.

When the system matrices are not independent of speed, there are several alternative methods which might be selected for evaluating the critical speeds as enumerated below, and demonstrated in the example. In many books the first two of these approaches are discussed, and they may be consulted for further details [16, 17, 19–24].

(1) For each speed in a set of speeds spanning the range of interest, the response of the machine to synchronous unbalance is computed. This involves computing the dynamic stiffness and finding the response to some nominal unbalance force for each speed, Ω, by solving equation (4). Peaks in the response are noted and recorded as "critical speeds". Clearly, this approach finds critical speeds as defined by using the "local maximum in response" criterion and these will not be exact solutions for equation (6). The approach is not able to find critical speeds that are not excited by the chosen unbalance. Furthermore, the frequency at which the response is maximum will change slightly depending on which DoF is considered.

(2) For each speed, Ω, in a set of speeds spanning the range of interest, mass, damping and stiffness matrices $\mathbf{M}(\Omega)$, $\mathbf{C}(\Omega)$, and $\mathbf{K}(\Omega)$ are set up and the characteristic roots of this combination of matrices are found by solving an eigenvalue problem such as equation (7). The imaginary parts of these characteristic roots are the damped resonance frequencies. A plot (called a Campbell diagram) can be created showing the variation of these resonance frequencies with shaft speed. The intersection of each resonance frequency curve with the line through the origin (on which shaft speed equals resonance frequency) defines a critical speed. This is the technique used (combined with (1) above when the damping is high) by Lalanne and Ferraris [16].

(3) An iterative search for critical speeds can be used to locate individual critical speeds. In this method, the first critical speed is estimated as Ω_1. Then $\mathbf{K}(\Omega_1)$, $\mathbf{C}(\Omega_1)$ and $\mathbf{M}(\Omega_1)$ are computed and equation (7) is solved to find the damped resonance frequencies. The lowest of these damped resonance frequencies is always an improved approximation to the first critical speed. Thus Ω_1 is given this new value and the process is repeated until satisfactory convergence is obtained. The numerical example illustrates this process in action and convergence is generally very fast. Higher critical speeds are obtained by choosing the higher damped resonance frequencies as a better approximation to the critical speed at each iteration.

(4) A method which could be referred to as *polynomial fit to bearing characteristics* could be applied to the problem. The present authors have not found any reference in the rotor-dynamics literature which specifically claims to use this approach but polynomial approximations have been used in modal analysis for some time [25]. Similar techniques have also been used to solve non-linear eigenvalue problems. Since the present authors hold this to be the principal contender with the new method proposed in this paper, a separate section is devoted to it. The formulation of this method also lays much of the useful foundation for the explanation of the proposed new method.

4. USING A POLYNOMIAL FIT TO BEARING CHARACTERISTICS

This method begins with the recognition that for the purposes of computing synchronous response or critical speeds, every (short) bearing can be characterized by a

single complex 2×2 dynamic stiffness matrix which relates the synchronous oscillatory forces existing in the oil film to the displacements of the shaft journal relative to the bearing shell. These dynamic stiffness matrices are assembled to the full bearing dynamic stiffness matrix, $\mathbf{B}(\Omega)$, as

$$\mathbf{B}(\Omega) = \begin{bmatrix} \hat{\mathbf{B}}_1(\Omega) & & & \\ & \hat{\mathbf{B}}_2(\Omega) & & \\ & & \ddots & \\ & & & \hat{\mathbf{B}}_m(\Omega) \end{bmatrix}, \tag{8}$$

where $\hat{\mathbf{B}}_i(\Omega)$ is the dynamic stiffness of the ith bearing, and there are m bearings. As indicated by equation (2), the force arising at the bearings depends on the relative displacement of the rotor and thus

$$\mathbf{f}_{F,B} = \mathbf{B}(\Omega)(\mathbf{u}_{R,B} - \mathbf{u}_{F,B}), \tag{9}$$

where the displacements and forces may also be partitioned according to their bearing location. We will continue using the general form, equation (9), although in practice the bearing dynamic stiffness matrix will be built up from the contributions from the individual bearings.

The bearing dynamic stiffness may be approximated by a polynomial in $j\Omega$ of arbitrary order n, where the rotor speed Ω is real. Thus,

$$\mathbf{B}(\Omega) \approx \mathbf{B}_0 + (j\Omega)\mathbf{B}_1 + (j\Omega)^2\mathbf{B}_2 + \cdots + (j\Omega)^n\mathbf{B}_n. \tag{10}$$

These coefficient matrices are usually obtained by minimizing the residuals between the polynomial expression for the bearing dynamic stiffness and the ones obtained by hydrodynamic theory (or possibly experiment), often in a least squares sense. It is worth noting that short hydrodynamic bearings are generally characterized by using four purely real stiffness coefficients and four purely real damping coefficients for a given shaft speed but that this representation is intended to be valid for all frequencies of lateral oscillations of the shaft and this paper is concerned only with synchronous oscillations. Thus, the bearing can be "characterized" at any one speed by using only four generally complex numbers.

If $n = 2$ in equation (10), then this polynomial expansion for the bearing coefficients can be used directly in equation (7) by recognizing that $\mathbf{B}_0$, $\mathbf{B}_1$ and $\mathbf{B}_2$ can be incorporated directly into $\mathbf{K}$, $\mathbf{C}$ and $\mathbf{M}$ respectively. Thus,

$$\mathbf{K} = \begin{bmatrix} \mathbf{K}_{R,II} & \mathbf{K}_{R,IB} & \mathbf{0} & \mathbf{0} \\ \mathbf{K}_{R,BI} & \mathbf{K}_{R,BB} + \mathbf{B}_0 & -\mathbf{B}_0 & \mathbf{0} \\ \mathbf{0} & -\mathbf{B}_0 & \mathbf{B}_0 + \mathbf{K}_{F,BB} & \mathbf{K}_{F,BI} \\ \mathbf{0} & \mathbf{0} & \mathbf{K}_{F,IB} & \mathbf{K}_{F,II} \end{bmatrix},$$

$$\mathbf{C} = \begin{bmatrix} \mathbf{C}_{R,II} & \mathbf{C}_{R,IB} & \mathbf{0} & \mathbf{0} \\ \mathbf{C}_{R,BI} & \mathbf{C}_{R,BB} + \mathbf{B}_1 & -\mathbf{B}_1 & \mathbf{0} \\ \mathbf{0} & -\mathbf{B}_1 & \mathbf{B}_1 + \mathbf{C}_{F,BB} & \mathbf{C}_{F,BI} \\ \mathbf{0} & \mathbf{0} & \mathbf{C}_{F,IB} & \mathbf{C}_{F,II} \end{bmatrix},$$

$$\mathbf{M} = \begin{bmatrix} \mathbf{M}_{R,II} & \mathbf{M}_{R,IB} & \mathbf{0} & \mathbf{0} \\ \mathbf{M}_{R,BI} & \mathbf{M}_{R,BB} + \mathbf{B}_2 & -\mathbf{B}_2 & \mathbf{0} \\ \mathbf{0} & -\mathbf{B}_2 & \mathbf{B}_2 + \mathbf{M}_{F,BB} & \mathbf{M}_{F,BI} \\ \mathbf{0} & \mathbf{0} & \mathbf{M}_{F,IB} & \mathbf{M}_{F,II} \end{bmatrix}. \tag{11}$$

Then when the dynamic stiffness matrix is formed for the complete machine including the bearing connections according to equation (4), it can be a reasonably close approximation to the exact matrix over a wide band of speeds. It is worth noting that $\mathbf{B}_0$, $\mathbf{B}_1$ and $\mathbf{B}_2$ are generally complex but the entries of the structural matrices arising from the rotor and foundation models are generally real. Complex entries sometimes appear in the stiffness matrices to represent hysteretic damping. The introduction of a small number of complex entries into the otherwise purely real matrices constitutes no significant computational disadvantage, but the resulting eigenvalues will not appear as complex conjugate pairs. If necessary the polynomial expansion in equation (10) can be forced to give purely real matrices $\mathbf{B}_0$, $\mathbf{B}_1$ and $\mathbf{B}_2$, although this will result in a considerable reduction in the quality of fit to the bearing characteristics. Once $\mathbf{K}$, $\mathbf{C}$ and $\mathbf{M}$ are defined, then equation (7) can be applied to find critical speeds. The roots of equation (7) are generally complex. If the system is lightly damped, it will be found that most of the roots are almost purely imaginary with a relatively small (negative) real part.

If $n = 3$ or $n = 4$ in equation (10), then the approximation to the exact $\mathbf{B}(\Omega)$ can be improved but the size of the matrices in the eigenvalue problem must be increased. Equations (12) show how the higher order polynomial fit can be incorporated into the framework of stiffness, damping and mass matrices:

$$\mathbf{K} = \begin{bmatrix} \mathbf{K}_{R,II} & \mathbf{K}_{R,IB} & \mathbf{0} & \mathbf{0} & \mathbf{0} \\ \mathbf{K}_{R,BI} & \mathbf{K}_{R,BB} + \mathbf{B}_0 & \mathbf{0} & -\mathbf{B}_0 & \mathbf{0} \\ \mathbf{0} & \mathbf{0} & \mathbf{I} & \mathbf{0} & \mathbf{0} \\ \mathbf{0} & -\mathbf{B}_0 & \mathbf{0} & \mathbf{B}_0 + \mathbf{K}_{F,BB} & \mathbf{K}_{F,BI} \\ \mathbf{0} & \mathbf{0} & \mathbf{0} & \mathbf{K}_{F,IB} & \mathbf{K}_{F,II} \end{bmatrix},$$

$$\mathbf{C} = \begin{bmatrix} \mathbf{C}_{R,II} & \mathbf{C}_{R,IB} & \mathbf{0} & \mathbf{0} & \mathbf{0} \\ \mathbf{C}_{R,BI} & \mathbf{C}_{R,BB} + \mathbf{B}_1 & \mathbf{B}_3 & -\mathbf{B}_1 & \mathbf{0} \\ \mathbf{0} & \mathbf{0} & \mathbf{0} & \mathbf{0} & \mathbf{0} \\ \mathbf{0} & -\mathbf{B}_1 & -\mathbf{B}_3 & \mathbf{B}_1 + \mathbf{C}_{F,BB} & \mathbf{C}_{F,BI} \\ \mathbf{0} & \mathbf{0} & \mathbf{0} & \mathbf{C}_{F,IB} & \mathbf{C}_{F,II} \end{bmatrix},$$

$$\mathbf{M} = \begin{bmatrix} \mathbf{M}_{R,II} & \mathbf{M}_{R,IB} & \mathbf{0} & \mathbf{0} & \mathbf{0} \\ \mathbf{M}_{R,BI} & \mathbf{M}_{R,BB} + \mathbf{B}_2 & \mathbf{B}_4 & -\mathbf{B}_2 & \mathbf{0} \\ \mathbf{0} & -\mathbf{I} & \mathbf{0} & \mathbf{I} & \mathbf{0} \\ \mathbf{0} & -\mathbf{B}_2 & -\mathbf{B}_4 & \mathbf{B}_2 + \mathbf{M}_{F,BB} & \mathbf{M}_{F,BI} \\ \mathbf{0} & \mathbf{0} & \mathbf{0} & \mathbf{M}_{F,IB} & \mathbf{M}_{F,II} \end{bmatrix}. \tag{12}$$

Notice that there is no advantage in considering only the cubic approximation in equation (10), as the size of the matrices is increased by the number of DoFs at the bearings, for both the cubic and quartic approximations to the bearing characteristics. In solving equation (7), it is necessary to find an inverse of $\mathbf{K}$ and $\mathbf{M}$ and therefore, it is desirable

to ensure that these matrices are always non-singular. It is useful to minimize the level of skew-symmetry in the matrices as this can reduce the computation time required to solve the eigenvalue problem [26].

In equations (12), additional entries have been introduced into the vector of system deflections $\mathbf{u}$. These additional deflection variables will be referred to as *dummy freedoms* and the positions at which they are introduced are arbitrary. There is some sense in introducing them at the partitions between the shaft translations and the bearing housing translations in the vector of deflections and this was done in the definitions in equations (12).

For $n = 6$, a second set of dummy freedoms may be introduced to give the mass, damping and stiffness matrices as

$$\mathbf{K} = \begin{bmatrix} \mathbf{K}_{R,II} & \mathbf{K}_{R,IB} & \mathbf{0} & \mathbf{0} & \mathbf{0} & \mathbf{0} \\ \mathbf{K}_{R,BI} & \mathbf{K}_{R,BB} + \mathbf{B}_0 & \mathbf{0} & \mathbf{0} & -\mathbf{B}_0 & \mathbf{0} \\ \mathbf{0} & \mathbf{0} & \mathbf{I} & \mathbf{0} & \mathbf{0} & \mathbf{0} \\ \mathbf{0} & \mathbf{0} & \mathbf{0} & \mathbf{I} & \mathbf{0} & \mathbf{0} \\ \mathbf{0} & -\mathbf{B}_0 & \mathbf{0} & \mathbf{0} & \mathbf{B}_0 + \mathbf{K}_{F,BB} & \mathbf{K}_{F,BI} \\ \mathbf{0} & \mathbf{0} & \mathbf{0} & \mathbf{0} & \mathbf{K}_{F,IB} & \mathbf{K}_{F,II} \end{bmatrix},$$

$$\mathbf{C} = \begin{bmatrix} \mathbf{C}_{R,II} & \mathbf{C}_{R,IB} & \mathbf{0} & \mathbf{0} & \mathbf{0} & \mathbf{0} \\ \mathbf{C}_{R,BI} & \mathbf{C}_{R,BB} + \mathbf{B}_1 & \mathbf{B}_3 & \mathbf{B}_5 & -\mathbf{B}_1 & \mathbf{0} \\ \mathbf{0} & \mathbf{0} & \mathbf{0} & \mathbf{0} & \mathbf{0} & \mathbf{0} \\ \mathbf{0} & \mathbf{0} & \mathbf{0} & \mathbf{0} & \mathbf{0} & \mathbf{0} \\ \mathbf{0} & -\mathbf{B}_1 & -\mathbf{B}_3 & -\mathbf{B}_5 & \mathbf{B}_1 + \mathbf{C}_{F,BB} & \mathbf{C}_{F,BI} \\ \mathbf{0} & \mathbf{0} & \mathbf{0} & \mathbf{0} & \mathbf{C}_{F,IB} & \mathbf{C}_{F,II} \end{bmatrix},$$

$$\mathbf{M} = \begin{bmatrix} \mathbf{M}_{R,II} & \mathbf{M}_{R,IB} & \mathbf{0} & \mathbf{0} & \mathbf{0} & \mathbf{0} \\ \mathbf{M}_{R,BI} & \mathbf{M}_{R,BB} + \mathbf{B}_2 & \mathbf{B}_4 & \mathbf{B}_6 & -\mathbf{B}_2 & \mathbf{0} \\ \mathbf{0} & -\mathbf{I} & \mathbf{0} & \mathbf{0} & \mathbf{I} & \mathbf{0} \\ \mathbf{0} & \mathbf{0} & -\mathbf{I} & \mathbf{0} & \mathbf{0} & \mathbf{0} \\ \mathbf{0} & -\mathbf{B}_2 & -\mathbf{B}_4 & -\mathbf{B}_6 & \mathbf{B}_2 + \mathbf{M}_{F,BB} & \mathbf{M}_{F,BI} \\ \mathbf{0} & \mathbf{0} & \mathbf{0} & \mathbf{0} & \mathbf{M}_{F,IB} & \mathbf{M}_{F,II} \end{bmatrix}. \tag{13}$$

A pattern may now be established whereby a polynomial approximation for the bearing coefficients of arbitrary degree can be created and installed into the system matrices to yield a direct and efficient calculation method for critical speeds. The approximation of the bearing characteristics are taken as even powers of rotational speed. Each increase of 2 in the order of the polynomial approximation requires the addition of N_b dummy freedoms, where N_b is the number of degrees of freedom at the bearing (that is the length of the vector $\mathbf{u}_{R,B}$).

5. THE ALTERNATIVE TECHNIQUE PROPOSED

The technique presented here can be expressed very concisely by reference to equations (11)–(13) above. In these equations, the dynamic properties of the bearing were represented by three matrics, **M**, **C**, and **K**. Dummy freedoms were introduced to derive these matrices,

but these dummy freedoms were essentially constrained to be even derivatives of the relative displacement of the bearing. Higher order polynomial approximations to the bearing characteristics increased the number of dummy freedoms and increased the accuracy of the approximation. The disadvantage is increased computation time. Furthermore complex matrices are required for a fully general polynomial fit to the bearing characteristics. The technique proposed in this paper delivers a greater accuracy than the polynomial expansion for the same computation time because it effectively allows more variables to be used in the definitions of the mass, damping and stiffness matrices. The resulting matrices are also real. This is done by allowing the dummy freedoms to have dynamics of their own. This essentially means adding general matrices into the corresponding positions in the mass, damping and stiffness matrices. Thus, one assumes these matrices may be written as

$$\mathbf{K} = \begin{bmatrix} \mathbf{K}_{R,II} & \mathbf{K}_{R,IB} & \mathbf{0} & \mathbf{0} & \mathbf{0} \\ \mathbf{K}_{R,BI} & \mathbf{K}_{R,BB} + \mathbf{B}_0 & \mathbf{R}_0 & -\mathbf{B}_0 & \mathbf{0} \\ \mathbf{0} & \mathbf{S}_0^{\mathrm{T}} & \mathbf{K}_D & -\mathbf{S}_0^{\mathrm{T}} & \mathbf{0} \\ \mathbf{0} & -\mathbf{B}_0 & -\mathbf{R}_0 & \mathbf{B}_0 + \mathbf{K}_{F,BB} & \mathbf{K}_{F,BI} \\ \mathbf{0} & \mathbf{0} & \mathbf{0} & \mathbf{K}_{F,IB} & \mathbf{K}_{F,II} \end{bmatrix},$$

$$\mathbf{C} = \begin{bmatrix} \mathbf{C}_{R,II} & \mathbf{C}_{R,IB} & \mathbf{0} & \mathbf{0} & \mathbf{0} \\ \mathbf{C}_{R,BI} & \mathbf{C}_{R,BB} + \mathbf{B}_1 & \mathbf{R}_1 & -\mathbf{B}_1 & \mathbf{0} \\ \mathbf{0} & \mathbf{S}_1^{\mathrm{T}} & \mathbf{C}_D & -\mathbf{S}_1^{\mathrm{T}} & \mathbf{0} \\ \mathbf{0} & -\mathbf{B}_1 & -\mathbf{R}_1 & \mathbf{B}_1 + \mathbf{C}_{F,BB} & \mathbf{C}_{F,BI} \\ \mathbf{0} & \mathbf{0} & \mathbf{0} & \mathbf{C}_{F,IB} & \mathbf{C}_{F,II} \end{bmatrix},$$

$$\mathbf{M} = \begin{bmatrix} \mathbf{M}_{R,II} & \mathbf{M}_{R,IB} & \mathbf{0} & \mathbf{0} & \mathbf{0} \\ \mathbf{M}_{R,BI} & \mathbf{M}_{R,BB} + \mathbf{B}_2 & \mathbf{R}_2 & -\mathbf{B}_2 & \mathbf{0} \\ \mathbf{0} & \mathbf{S}_2^{\mathrm{T}} & \mathbf{M}_D & -\mathbf{S}_2^{\mathrm{T}} & \mathbf{0} \\ \mathbf{0} & -\mathbf{B}_2 & -\mathbf{R}_2 & \mathbf{B}_2 + \mathbf{M}_{F,BB} & \mathbf{M}_{F,BI} \\ \mathbf{0} & \mathbf{0} & \mathbf{0} & \mathbf{M}_{F,IB} & \mathbf{M}_{F,II} \end{bmatrix}, \tag{14}$$

where the bearing characteristics are now approximated by the identified values in the matrices in the following equation:

$$\mathbf{B}(\Omega) \approx \mathbf{B}_0 + \mathrm{j}\Omega\mathbf{B}_1 + (\mathrm{j}\Omega)^2\mathbf{B}_2 - [\mathbf{R}_0 + \mathrm{j}\Omega\mathbf{R}_1 + (\mathrm{j}\Omega)^2\mathbf{R}_2]\,[\mathbf{K}_D + \mathrm{j}\Omega\mathbf{C}_D + (\mathrm{j}\Omega)^2\mathbf{M}_D]^{-1} \times [\mathbf{S}_0 + \mathrm{j}\Omega\mathbf{S}_1 + (\mathrm{j}\Omega)^2\mathbf{S}_2]^{\mathrm{T}}. \tag{15}$$

Equations (14) and (15) are the most general expressions for the structural matrices, consistent with the constraint that the forces on each side of the bearings are equal in magnitude, but opposite in direction. The number of dummy DoFs used determines the size of the mass, damping and stiffness matrices, $\mathbf{M}_D$, $\mathbf{C}_D$ and $\mathbf{K}_D$. This number is determined solely by the quality of fit to the bearing characteristics required. It should be clear from equation (15) that the wider choice of parameters enables a much closer approximation to be made to the bearing characteristics than could be obtained with a polynomial fit.

Although the mass, damping and stiffness matrices for the dummy freedoms, $\mathbf{M}_D$, $\mathbf{C}_D$ and $\mathbf{K}_D$, can take any form, these degrees of freedom are not physical, and therefore may

be transformed arbitrarily. One particular convenient form is to assume that the dummy freedoms are such that these matrices are diagonal. This form assumes proportional damping, whereas the most general form retains a full damping matrix. In practice, a good fit to the bearing characteristics may be obtained by assuming proportional damping, and this assumption will be used in the example to follow. Thus, if there are p dummy freedoms, and if

$$\mathbf{M}_D = \text{diag}\,([m_{D1}, m_{D2}, \ldots, m_{Dp}]), \qquad \mathbf{C}_D = \text{diag}\,([c_{D1}, c_{D2}, \ldots, c_{Dp}]),$$

$$\mathbf{K}_D = \text{diag}\,([k_{D1}, k_{D2}, \ldots, k_{Dp}]),$$

then equations (15) may be written as

$$\mathbf{B}(\Omega) \approx \mathbf{B}_0 + \mathrm{j}\Omega\mathbf{B}_1 + (\mathrm{j}\Omega)^2\mathbf{B}_2 - \sum_{i=1}^{p} \frac{\{k_{Di}\,\mathbf{r}_{0i} + \mathrm{j}\Omega c_{Di}\,\mathbf{r}_{1i} + (\mathrm{j}\Omega)^2\mathbf{r}_{2j}\}\,\{k_{Di}\,\mathbf{s}_{0i} + \mathrm{j}\Omega c_{Di}\,\mathbf{s}_{1i} + (\mathrm{j}\Omega)^2\mathbf{s}_{2i}\}^{\mathrm{T}}}{k_{Di} + \mathrm{j}\Omega c_{Di} + (\mathrm{j}\Omega)^2}, \tag{16}$$

where the $\mathbf{R}$ and $\mathbf{S}$ matrices have been written as

$$\mathbf{R}_0 = [k_{Di}\,\mathbf{r}_{01} \quad k_{D2}\,\mathbf{r}_{02} \quad \cdots \quad k_{Dp}\,\mathbf{r}_{0p}], \qquad \mathbf{S}_0 = [k_{D1}\,s_{01} \quad k_{D2}\,\mathbf{s}_{02} \quad \cdots \quad k_{Dp}\,\mathbf{s}_{0p}],$$

$$\mathbf{R}_1 = [c_{D1}\,\mathbf{r}_{11} \quad c_{D2}\,\mathbf{r}_{12} \quad \cdots \quad c_{Dp}\,\mathbf{r}_{1p}], \qquad \mathbf{S}_1 = [c_{D1}\,\mathbf{s}_{11} \quad c_{D2}\,\mathbf{s}_{12} \quad \cdots \quad c_{Dp}\,\mathbf{s}_{1p}],$$

$$\mathbf{R}_2 = [\mathbf{r}_{21} \quad \mathbf{r}_{22} \quad \cdots \quad \mathbf{r}_{2p}], \qquad \mathbf{S}_2 = [\mathbf{s}_{21} \quad \mathbf{s}_{22} \quad \cdots \quad \mathbf{s}_{2p}].$$

Since each numerator and denominator pair in equation (16) may be multiplied by any scalar constant, one may arbitrarily set $m_{Di} = 1$.

The question that now arises is how to choose the parameters relating to the dummy freedoms so that the bearing dynamic stiffness matrix is closely approximated by the expression in equation (16). Methods based on the direct minimization of the residual in equation (16) will give significant problems as the error surface that is minimized has many local minima. Indeed the direct approach has been abandoned in experimental modal analysis, which is essentially looking at the same problem. In the standard frequency domain modal analysis method one fits a rational fraction polynomial expression to the dynamic stiffness matrix, and this yields as a first stage the natural frequencies and damping ratios [27]. This approach may be used here to obtain the denominator terms in equation (16).

It remains to estimate the $\mathbf{R}$ and $\mathbf{S}$ matrices. Equation (16) may be rewritten in the form

$$\mathbf{B}(\Omega) \approx \mathbf{T}_0 + \mathrm{j}\Omega\mathbf{T}_1 + (\mathrm{j}\Omega)^2\mathbf{T}_2 - \sum_{i=1}^{p} \frac{\mathbf{T}_{3i} + \mathrm{j}\Omega\mathbf{T}_{4i}}{k_{Di} + \mathrm{j}\Omega c_{Di} + (\mathrm{j}\Omega)^2}, \tag{17}$$

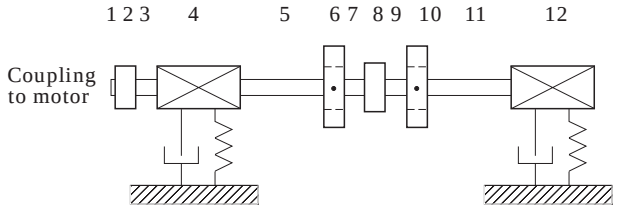

Figure 1. Diagram of the rotor for the numerical example.

where the **T** matrices may be written in terms of the **B**, **S** and **R** matrices. This is the form of the model that may be easily identified by the rational fraction polynomial method. The matrices **R** and **S** then have to be computed so that the numerator terms in the summations in equations (16) and (17) are equal. Then the **B** matrices in equation (16) may be found by equating the quadratic terms in equations (16) and (17). Matching the numerator terms, after considerable algebra, gives the following conditions that the **R** and **S** matrices must satisfy:

$$k_{Di}\{\mathbf{r}_{2i}-\mathbf{r}_{0i}\}\{\mathbf{s}_{2i}-\mathbf{s}_{0i}\}^{\mathrm{T}}-c_{Di}^2\{\mathbf{r}_{1i}-\mathbf{r}_{0i}\}\{\mathbf{s}_{1i}-\mathbf{s}_{0i}\}^{\mathrm{T}}=\frac{k_{Di}-c_{Di}^2}{k_{Di}^2}\mathbf{T}_{3i}+\frac{c_{Di}}{k_{Di}}\mathbf{T}_{4i}, \tag{18}$$

$$\{\mathbf{r}_{2i}-\mathbf{r}_{1i}\}\{\mathbf{s}_{2i}-\mathbf{s}_{1i}\}^{\mathrm{T}}-\{\mathbf{r}_{1i}-\mathbf{r}_{0i}\}\{\mathbf{s}_{1i}-\mathbf{s}_{0i}\}^{\mathrm{T}}=-\frac{1}{k_{Di}^2}\mathbf{T}_{3i}+\frac{1}{c_{Di}k_{Di}}\mathbf{T}_{4i}. \tag{19}$$

It is clear that the left sides of equations (18) and (19), obtained from equation (16), will not be full rank in general, but of rank at most 2. The right sides of equations (18) and (19), involving the measured matrices $\mathbf{T}_{3i}$ and $\mathbf{T}_{4i}$, will in general be full rank. Thus the model using the dummy freedoms cannot be made equivalent to a model identified from the rational fraction polynomial method. However, if $\mathbf{B}(\Omega)$ represents a single short bearing, the matrices $\mathbf{T}_{3i}$ and $\mathbf{T}_{4i}$ will be 2×2, and therefore of rank at most 2. Even so, solutions for the **R** and **S** matrices from equations (18) and (19) are unlikely, and this is considered in more detail later. There is, of course, some redundancy in these equations, and in the following $\mathbf{r}_{2i}$ and $\mathbf{s}_{2i}$ will be set to zero. Upon assuming the **R** and **S** matrices have been found, then the **B** matrices may be obtained from the fitted constant, linear and quadratic terms: that is, $\mathbf{T}_{0i}$, $\mathbf{T}_{1i}$ and $\mathbf{T}_{2i}$, and also the **R** and **S** matrices. If there is more than one bearing, each bearing will be assumed to have its own dynamics, and therefore

TABLE 1

Physical dimensions and properties for the numerical example

Shaft properties				
Station	Length (mm)	Diameter (mm)	Young's modulus, E (GPa)	Mass density, ρ (kg m^{-3})
1	6·35	38·1	200	7850
2	25·4	77·6	200	7850
3	50·8	38·1	200	7850
4	203·2	100·0	200	7850
5	177·8	38·1	200	7850
6	50·8	116·8	200	7850
7	76·2	38·1	200	7850
8	76·2	109·7	200	7850
9	76·2	38·1	200	7850
10	50·8	102·9	200	7850
11	177·8	38·1	200	7850
12	203·2	100·0	200	7850

Balancing discs			
Station	Length (mm)	Diameter (mm)	Mass density, ρ (kg m^{-3})
6	25·4	203·2	7850
10	25·4	203·2	7850

dummy freedoms, and the bearing characteristics for the complete rotor may be generated in block diagonal form.

If the number of degrees of freedom in each bearing is larger than the rank of the $\mathbf{T}_{3i}$ and $\mathbf{T}_{4i}$ matrices, or there is no solution of equations (18) and (19), then the identified rational polynomial form cannot be used directly. There are then two possibilities. Either an optimization process is performed to generate the **B**, **R** and **S** matrices directly, by using the denominator polynomial identified from the rational fraction polynomial method. Direct optimization often has considerable difficulties and should be avoided if at all possible. The alternative is to add more dummy freedoms with the same "natural frequency" and "damping ratio": that is, the same denominator polynomial. This has the effect of making $\mathbf{r}_{qi}$ and $\mathbf{s}_{qi}$, $q = 0, 1, 2$, have more than one column. Thus the rank of the left sides of equations (18) and (19) may be increased. Dummy freedoms may be added until the rank of these matrices is equal to that of the equivalent measured matrices. This will now be demonstrated for short bearings, and a decomposition method introduced to produce the **R** and **S** matrices.

For short bearings it is required to add a second set of dummy degrees of freedom with the same "natural frequency" "damping ratio". For the ith dummy freedom, let the extra columns of the **R** and **S** matrices be denoted by $\hat{\mathbf{r}}_{qi}$ and $\hat{\mathbf{s}}_{qi}$, $q = 0, 1, 2$. On the assumption that

$$\hat{\mathbf{s}}_{2i} = \mathbf{s}_{2i} = \mathbf{0}, \qquad \hat{\mathbf{r}}_{2i} = \mathbf{r}_{2i} = \mathbf{0}, \tag{20}$$

equations (18) and (19) become

$$k_{Di}\,\mathbf{r}_{0i}\,\mathbf{s}_{0i}^{\mathrm{T}} - c_{Di}^2\,\{\mathbf{r}_{1i} - \mathbf{r}_{0i}\}\,\{\mathbf{s}_{1i} - \mathbf{s}_{0i}\}^{\mathrm{T}} + k_{Di}\,\hat{\mathbf{r}}_{0i}\,\hat{\mathbf{s}}_{0i}^{\mathrm{T}} - c_{Di}^2\,\{\hat{\mathbf{r}}_{1i} - \hat{\mathbf{r}}_{0i}\}\,\{\hat{\mathbf{s}}_{1i} - \hat{\mathbf{s}}_{0i}\}^{\mathrm{T}}$$
$$= (k_{Di} - c_{Di}^2)/k_{Di}^2\,\mathbf{T}_{3i} + (c_{Di}/k_{Di})\mathbf{T}_{4i}, \tag{21}$$

$$\mathbf{r}_{1i}\,\mathbf{s}_{1i}^{\mathrm{T}} - \{\mathbf{r}_{1i} - \mathbf{r}_{0i}\}\,\{\mathbf{s}_{1i} - \mathbf{s}_{0i}\}^{\mathrm{T}} + \hat{\mathbf{r}}_{1i}\,\hat{\mathbf{s}}_{1i}^{\mathrm{T}} - \{\hat{\mathbf{r}}_{1i} - \hat{\mathbf{r}}_{0i}\}\,\{\hat{\mathbf{s}}_{1i} - \hat{\mathbf{s}}_{0i}\}^{\mathrm{T}} = -1/k_{Di}^2\,\mathbf{T}_{3i} + 1/(c_{Di}\,k_{Di})\mathbf{T}_{4i}. \tag{22}$$

It happens that one does not need all the vectors (or columns of the **R** and **S** matrices) to be independent, and thus the following assignments can be made:

$$\hat{\mathbf{s}}_{0i} = \mathbf{s}_{0i}, \qquad \hat{\mathbf{s}}_{1i} = -\mathbf{s}_{1i}. \tag{23}$$

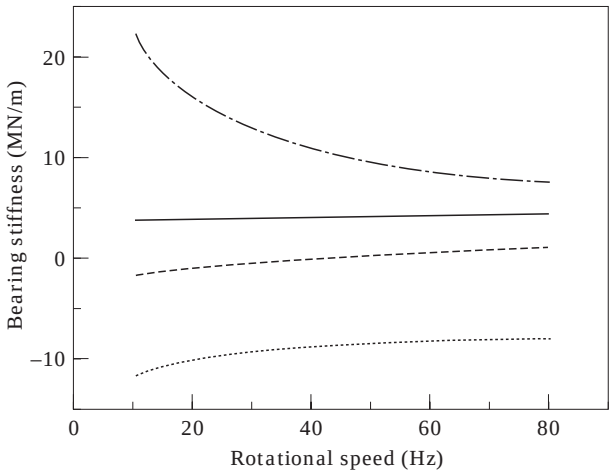

Figure 2. The speed dependent stiffness coefficients for the bearings used in the example. ——, (1, 1) element, · · · · ·, (2, 1) element; - - - -, (1, 2) element; — · — · , (2, 2) element.

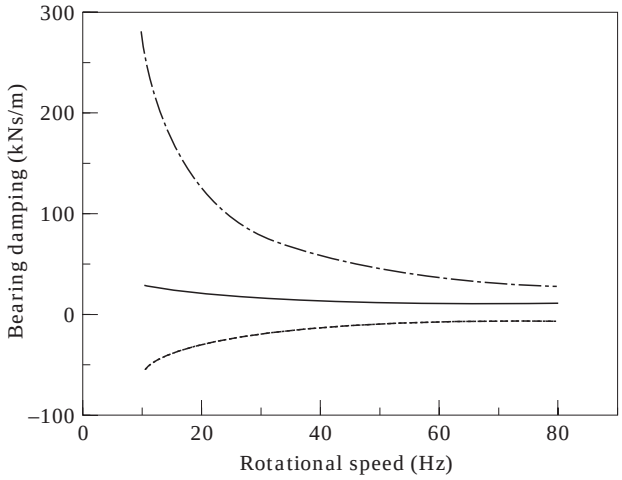

Figure 3. As Figure 2 but for the damping coefficients.

These assignments are not unique, and the only requirement is that the linear relationships in equations (23) have distinct coefficients. With these definitions, equations (21) and (22) become

$$\left[\begin{array}{c|c} k_{Di}\{\mathbf{r}_{0i}+\hat{\mathbf{f}}_{0i}\}+c_{Di}^2\{-\mathbf{r}_{0i}+\mathbf{r}_{1i}-\hat{\mathbf{f}}_{0i}+\hat{\mathbf{f}}_{1i}\} & c_{Di}^2\{\mathbf{r}_{0i}-\mathbf{r}_{1i}-\hat{\mathbf{f}}_{0i}+\hat{\mathbf{f}}_{1i}\} \\ \hline -\mathbf{r}_{0i}+\mathbf{r}_{1i}-\hat{\mathbf{f}}_{0i}+\hat{\mathbf{f}}_{1i} & \hat{\mathbf{f}}_{0i}-\hat{\mathbf{f}}_{0i} \end{array}\right]\left[\begin{array}{c}\mathbf{s}_{0i}^{\mathrm{T}}\\ \mathbf{s}_{1i}^{\mathrm{T}}\end{array}\right]$$

$$=\left[\begin{array}{c} \dfrac{k_{Di}-c_{Di}^2}{k_{Di}^2}\,\mathbf{T}_{3i}+\dfrac{c_{Di}}{k_{Di}}\,\mathbf{T}_{4i} \\ -\dfrac{1}{k_{Di}^2}\,\mathbf{T}_{3i}+\dfrac{1}{c_{Di}\,k_{Di}}\,\mathbf{T}_{4i} \end{array}\right]. \tag{24}$$

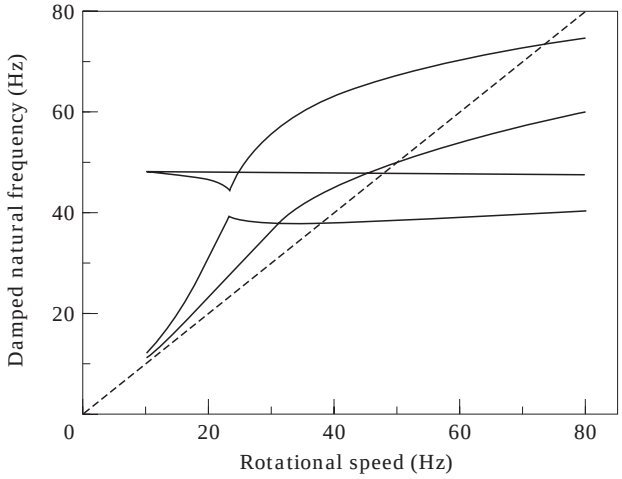

Figure 4. Campbell diagram for the numerical example.

It is now clear how the unknown vectors may be obtained. A singular value decomposition of the right side of equation (24) is performed. The right side has dimension 4×2 for short bearings, and the singular values are distributed equally by multiplying the left and right singular vectors by the square root of the corresponding singular values. The resulting matrix of "normalized" right singular vectors immediately gives the **s** vectors. The "normalized" left hand singular vectors are contained in a 4×2 matrix, and this gives 8 linear equations for the 8 unknown elements of the **r** vectors. This approach may be extended to matrices of larger dimension and also for extra dummy degrees of freedom.

6. A NUMERICAL EXAMPLE

The numerical example is based on a small test rig located at Aston University, Birmingham. No experimental results are used since the purpose of this paper is to compare methods of calculating critical speeds, not to test the quality of the modelling. However, the example does show the calculation of critical speeds for a real system. The rig consists of a steel shaft approximately 1·1 m long, with nominal diameter 38 mm and two shrink-fitted balancing discs. The shaft is supported at either end by a journal bearing of diameter 100 mm, L/D ratio of 0·3 and radial clearance of 125 μm. The bearings contain oil with a viscosity of 0·0009 Nsm^{-2} and are supported on rigid pedestals. Each bearing is assumed to support a force of 300 N. The rig is designed to operate with a flexible foundation, but rigid pedestals are assumed here to highlight the speed dependent bearing properties, and hence speed dependent resonances. A schematic of the rig, as modelled, is shown in Figure 1. The dimensions of each station and material properties are given in Table 1. A finite element model of the rotor with 23 elements was created, with 4 DoFs per node (2 lateral translations and 2 rotations), resulting in a 96 DoFs model of the rotor. The rotor was assumed to be constrained along the axial direction of the rotor. The rotational DoFs in this model were eliminated by using Guyan reduction, giving a 48 DoFs model of the rotor. Short bearing theory was used to obtain values for the bearing stiffness and damping [28]. Figures 2 and 3 show the speed dependent bearing properties, given as stiffness and damping matrices, used in the simulation. Direction 1 is horizontal and direction 2 is vertical.

Figure 4 shows the Campbell diagram for this example, for rotor speeds up to 80 Hz, clearly showing four critical speeds in this range. Applying the iterative method to obtain the critical speed gives the results shown in Table 2. The initial guesses for the critical

TABLE 2

Convergence of critical speeds for the iterative method

Iteration no.	Critical speed (Hz)			
Initial	40·0000	48·0000	50·0000	74·0000
1	38·1220	48·0121	50·2166	73·4895
2	38·0440	48·0119	50·3138	73·3875
3	38·0410	48·0119	50·3572	73·3670
4	38·0409	—	50·3766	73·3629
5	38·0408	—	50·3852	73·3620
6	38·0408	—	50·3890	73·3619
7	—	—	50·3907	73·3618
8	—	—	50·3915	73·3618
9	—	—	50·3918	—
10	—	—	50·3920	—

TABLE 3

Estimated critical speeds, Ω_{crit}, and damping ratios, ζ, obtained by using the iterative method and the proposed method with different numbers of dummy DoFs

Iterative		8 Dummy DoFs		12 Dummy DoFs		16 Dummy DoFs		20 Dummy DoFs	
Ω_{crit} (Hz)	ζ (%)	Ω_{crit} (Hz)	ζ (%)	Ω_{crit} (Hz)	ζ (%)	Ω_{crit} (Hz)	ζ (%)	Ω_{crit} (Hz)	ζ (%)
38·04	13·0	39·11	12·1	39·13	12·1	39·13	12·1	39·13	12·1
48·01	2·3	47·99	2·2	48·00	2·2	47·99	2·2	47·99	2·2
50·39	32·6	60·70	32·1	60·74	32·0	60·71	32·0	60·71	32·0
73·36	17·2	76·66	19·2	76·61	19·2	76·62	19·2	76·62	19·2

speeds are obtained from the Campbell diagram and convergence is very fast. Table 3 shows the converged critical speeds, and also the corresponding damping ratios. Table 3 also shows the critical speeds obtained by using the new approach proposed in this paper, together with the corresponding damping ratios, for different numbers of dummy DoFs. In all cases the quality of the fit to the bearing characteristics was very good. The fitted characteristics are not shown because little error would be visible in plots equivalent to Figures 2 and 3. The number of dummy DoFs is the number of extra DoFs required, in addition to the 48 rotor DoFs. Only critical speeds inside the frequency range used to fit the bearing characteristics are shown in Table 3. Since the bearing model is not valid outside this range, critical speeds outside the range must be treated with great suspicion. These "numerical" or non-physical critical speeds may also be identified as they tend to change as the number of dummy DoFs varies and they are often highly damped, although in this example there are none. The correspondence between the critical speeds obtained by the iterative approach and the new approach is good for lightly damped critical speeds, and gets poorer as the damping ratio for a critical speed increases. Thus, the correspondence in the third critical speed is particularly poor because the damping ratio (32%) is very high. This poor correspondence arises because of the approximation inherent in the calculation of the critical speed via system eigenvalues, namely that the eigenvalue is equal to j times the critical speed (where $j = \sqrt{-1}$). Clearly this relies on the damping being small. The definition of critical speeds in highly damped systems was discussed earlier in this paper. To highlight the effect of this approximation, Table 4 shows the corresponding results for this example if the bearing damping is reduced by a factor of 2. The damping in all critical speeds is now small, and the correspondence between critical speeds is much improved.

TABLE 4

Estimated critical speeds, Ω_{crit}, and damping ratios, ζ, obtained by using the iterative method and the proposed method with different numbers of dummy DoFs; bearing damping reduced by a factor of 2

Iterative		8 Dummy DoFs		12 Dummy DoFs		16 Dummy DoFs		20 Dummy DoFs	
Ω_{crit} (Hz)	ζ (%)	Ω_{crit} (Hz)	ζ (%)	Ω_{crit} (Hz)	ζ (%)	Ω_{crit} (Hz)	ζ (%)	Ω_{crit} (Hz)	ζ (%)
39·30	1·5	39·35	1·7	39·35	1·6	39·35	1·6	39·35	1·6
47·28	2·6	47·26	2·5	47·26	2·5	47·26	2·5	47·26	2·5
68·26	1·2	68·52	1·5	68·53	1·5	68·53	1·5	68·53	1·5
83·59	0·23	83·66	0·28	83·64	0·26	83·63	0·26	83·63	0·26

TABLE 5

Estimated critical speeds, Ω_{crit}, and damping ratios, ζ, obtained by using the iterative method and a polynomial fit for different polynomial degree

Iterative		Polynomial degree = 2 0 Extra DoFs		Polynomial degree = 4 4 Extra DoFs		Polynomial degree = 6 8 Extra DoFs	
Ω_{crit} (Hz)	ζ (%)	Ω_{crit} (Hz)	ζ (%)	Ω_{crit} (Hz)	ζ (%)	Ω_{crit} (Hz)	ζ (%)
38·04	13·0	28·82	20·4	17·48	91·0	13·05	39·5
48·01	2·3	32·32	33·7	18·02	90·1	13·17	41·5
50·39	32·6	39·12	12·0	18·62	37·3	17·59	96·9
73·36	17·2	47·99	2·3	18·92	42·3	17·78	97·0
—	—	48·36	−0·6	22·83	−89·7	39·14	12·1
—	—	57·71	12·6	23·37	−89·1	47·99	2·2
—	—	58·46	32·4	39·13	12·2	48·68	0·0
—	—	64·47	72·9	47·99	2·2	49·34	1·4
—	—	64·91	71·6	48·61	0·0	52·85	63·9
—	—	75·61	21·3	50·92	4·9	55·80	61·7
—	—	—	—	61·63	30·2	59·91	−60·2
—	—	—	—	75·59	18·8	60·48	−59·3
—	—	—	—	—	—	60·65	33·6
—	—	—	—	—	—	76·70	18·2

For comparison, Tables 5 and 6 show the equivalent results obtained by fitting a polynomial to the bearing characteristics, and using the method outlined in section 4. Complex coefficient matrices are used and in all cases the curve fit is of high quality. The

TABLE 6

Estimated critical speeds, Ω_{crit}, and damping ratios, ζ, obtained by using the iterative method and a polynomial fit for different polynomial degree; bearing damping reduced by a factor of 2

Iterative		Polynomial degree = 2 0 Extra DoFs		Polynomial degree = 4 4 Extra DoFs		Polynomial degree = 6 8 Extra DoFs	
Ω_{crit} (Hz)	ζ (%)	Ω_{crit} (Hz)	ζ (%)	Ω_{crit} (Hz)	ζ (%)	Ω_{crit} (Hz)	ζ (%)
39·30	1·5	29·97	9·7	19·21	89·6	12·69	98·6
47·28	2·6	36·47	17·2	19·48	89·1	13·24	98·4
68·26	1·2	39·36	1·6	21·53	19·4	15·44	21·7
83·59	0·23	47·24	2·6	22·93	23·2	15·87	23·2
—	—	48·30	−0·2	23·17	−88·1	39·35	1·6
—	—	60·74	6·9	23·56	−87·4	47·26	2·5
—	—	65·32	63·3	39·34	1·6	48·68	0·0
—	—	67·51	62·1	47·27	2·5	49·75	1·0
—	—	68·23	1·5	48·60	0·0	52·38	62·4
—	—	85·48	1·8	52·43	3·6	52·40	62·4
—	—	—	—	59·98	−93·8	58·87	−58·4
—	—	—	—	60·91	−93·4	59·40	−57·0
—	—	—	—	68·39	1·4	68·55	1·5
—	—	—	—	82·34	4·1	84·09	0·5
—	—	—	—	84·59	0·9	—	—

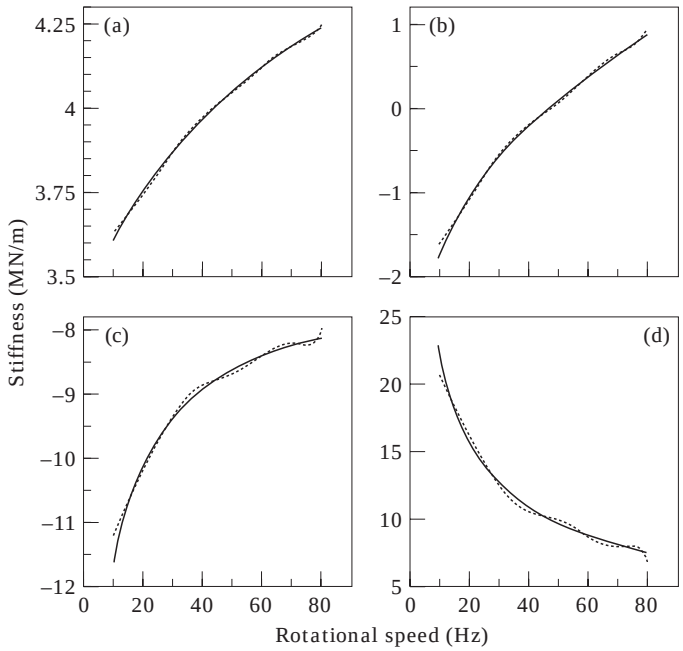

Figure 5. The fitted speed dependent stiffness coefficients obtained by using a polynomial of degree 10 with real coefficients, the dashed lines are the fitted data. Elements: (a) (1, 1); (b) (1, 2); (c) (2, 1); (d) (2, 2).

use of complex coefficient matrices means that the eigenvalues will not occur in complex conjugate pairs. This is one reason for the increased number of candidate critical speeds in the frequency range of interest. As the degree of the polynomial changes the true critical

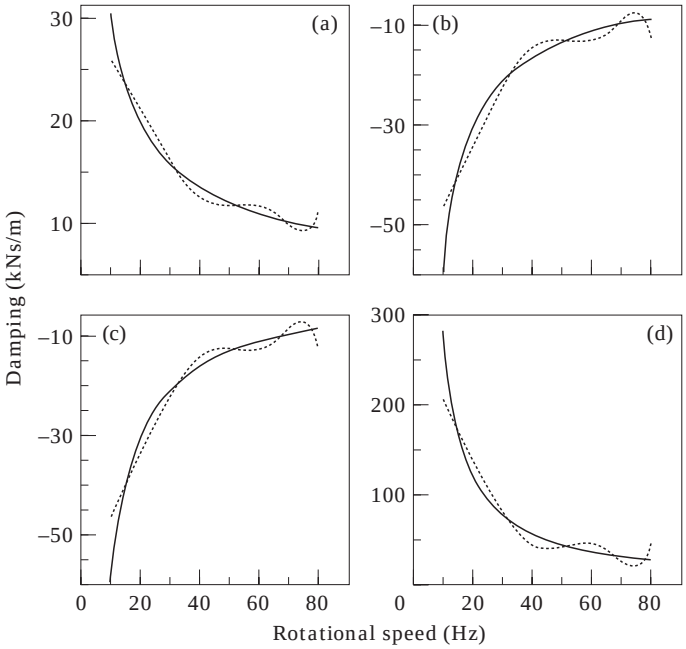

Figure 6. As Figure 5 but for the damping coefficients.

speeds remain quite constant, and correspond quite closely with those obtained from the proposed method, and given in Tables 3 and 4. However, there are a huge number if "numerical" or non-physical critical speeds, that must be investigated further and eliminated. For complex, large scale rotor-bearing systems this is likely to be very difficult. Figures 5 and 6 show the fit to the bearing characteristics, obtained by using real coefficients and a polynomial degree of 10. Despite the high polynomial degree the fit is very poor. This arises because the stiffness is modelled by using only even powers of rotor speed, and the damping by only odd powers. A huge number of potential critical speeds arise in this case because of the high polynomial degree required for a good fit, even though the eigenvalues now occur in complex conjugate pairs.

7. CONCLUSIONS

A new method for calculating critical speeds of rotating machines has been presented in which the speed-dependent characteristics of the bearings is incorporated by introducing dummy degrees of freedom between the rotor and the pedestals. This concept makes possible the accurate computation of all critical speeds of the machine after the solution of only one eigenvalue problem. The dimension of the matrices involved in this eigenvalue problem is only slightly greater than the dimension of matrices in the eigenvalue problem which is commonly solved for each of a relatively large number of rotor speeds in the standard procedure for computing critical speeds by developing the Campbell diagram.

Although the dramatic increases in available computation power have been such that the computation of critical speeds of a single machine design is now a comparatively trivial exercise, the computation requirements become significant again when the calculation procedure is embedded in design optimization studies, when it is used in model based diagnostics of rotating machines or when it is used repeatedly in certain classes of parameter identification methods. In these circumstances, the present method offers substantial advantage. It is self-evident that methods which require numerous solutions of large eigenvalue problems will be notably less efficient than those which require only one, provided the matrix dimensions in each case are not dissimilar.

The method has been compared closely with an extension of an established mathematical technique involving the use of polynomial fits to the speed dependent properties. Though the polynomial fit method itself appears not to be commonly used in the analysis of rotating machines, this approach has been used in areas such as experimental modal analysis and the solution of non-linear eigenvalue problems, and is the closest rival to the proposed technique for computational efficiency. However the polynomial approximation introduces extra, non-physical modes that must be identified and discarded, making the proposed technique much more efficient in practice.

ACKNOWLEDGMENT

Dr. Friswell gratefully acknowledges the support of the Engineering and Physical Sciences Research Council through the award of an Advanced Fellowship.

REFERENCES

1. M. Rajan, S. D. Rajan, H. D. Nelson and W. J. Chen 1987 *ASME Journal of Vibration, Acoustics, Stress, and Reliability in Design* **109**, 152–157. Optimal placement of critical speeds in rotor-bearing systems.

2. T. N. Shiau and J. R. Chang 1993 *ASME Journal for Gas Turbines and Power* **115**, 246–255. Multi-objective optimization of rotor-bearing system with critical speed constraints.
3. N. O. Myklestad 1944 *Journal of the Aeronautical Sciences* **11**, 176–178. A new method of calculating uncoupled bending vibration of airplane wings and other types of beam.
4. M. A. Prohl 1945 *Journal of Applied Mechanics* **12**, A142–A148. A general method for calculating the critical speeds of flexible rotors.
5. R. Firoozian and H. Zhu 1991 *IMechE Journal of Mechanical Engineering Science* **205**, 131–137. A hybrid method for the vibration analysis of rotor-bearing systems.
6. J. Gu 1986 *ASME Journal of Vibration*, *Acoustics*, *Stress and Reliability in Design* **108**, 182–188. An improved transfer matrix–direct integration method for rotor dynamics.
7. J. M. Vance, B. T. Murphy and H. A. Tripp 1987 *ASME Journal of Vibration*, *Acoustics*, *Stress and Reliability in Design* **109**, 1–7. Critical speeds of turbomachinery: computer predictions vs. experimental measurements—part I: the rotor mass–elastic model.
8. J. M. Vance, B. T. Murphy and H. A. Tripp 1987 *ASME Journal of Vibration*, *Acoustics*, *Stress and Reliability in Design* **109**, 8–14. Critical speeds of turbomachinery: computer predictions vs. experimental measurements—part II: effect of tilt-pad bearings and foundation dynamics.
9. J. W. Lund and Z. Wang 1986 *ASME Journal of Vibration*, *Acoustics*, *Stress and Reliability in Design* **108**, 177–181. Application of the Ricatti method to rotor dynamic analysis of long shafts on a flexible foundation.
10. J. W. Lund 1974 *ASME Journal of Engineering for Industry* **96**, 509–517. Stability and damped critical speeds of a flexible rotor in fluid-film bearings.
11. N. Feng, E. J. Hahn, A. Lattab and A. Sestieri 1992 *IMechE International Conference on Vibrations in Rotating Machinery*, 529–534. A combined finite-element/transfer-matrix approach for including foundation effects on the vibration behaviour of rotating machinery.
12. R. L. Ruhl and J. F. Booker 1986 *ASME Journal of Vibration*, *Acoustics*, *Stress and Reliability in Design* **108**, 177–181, paper C432/142. A finite element model for distributed parameter turborotor systems.
13. V. Ramamurty and A. R. P. Simah 1987 *Journal of Sound and Vibration* **117**, 578–582. Finite element calculation of critical speeds of rotation of shafts with gyroscopic action of discs.
14. R. Firoozian and R. Stanway 1989 *Journal of Sound and Vibration* **134**, 115–137. Design and application of a finite element package for modelling turbomachinery vibrations.
15. A. D. Dimaragonas 1992 *Vibration for Engineers*. Englewood Heights NJ: Prentice-Hall.
16. M. Lalanne and G. Ferraris 1998 *Rotordynamics Prediction in Engineering*. New York; John Wiley: second edition.
17. D. Childs 1993 *Turbomachinery Rotordynamics*: *Phenomena*, *Modeling*, *and Analysis*. New York: John Wiley.
18. R. J. Iannuzzelli 1985 *Journal of Machine Design* **25**, 83–96. Avoiding errors in critical speed predictions.
19. G. Genta 1993 *Vibration of Structures and Machines*: *Practical Aspects*. Berlin: Springer-Verlag.
20. A. D. Dimaragonas and S. A. Paipetis 1983 *Analytical Methods in Rotor Dynamics*. Amsterdam: Elsevier Applied Science.
21. J. M. Vance 1988 *Rotordynamics of Turbomachinery*. New York: John Wiley.
22. J. S. Rao 1983 *Rotor Dynamics*. New York: John Wiley.
23. F. F. Ehrich (editor) 1992 *Handbook of Rotordynamics*. New York: McGraw-Hill.
24. E. Krämer 1993 *Dynamics of Rotors and Foundations*. Berlin: Springer-Verlag.
25. H. Van der Auweraer and J. Leuridan 1987 *Mechanical Systems and Signal Processing* **1**, 259–272. Multiple input orthogonal polynomial parameter-estimation.
26. S. D. Garvey 1993 *International Journal for Numerical Methods in Engineering* **36**, 4151–4163. An efficient method for solving the eigenvalue problem for matrices having a skew-symmetrical (or skew-Hermitian) component of low rank.
27. M. I. Friswell and J. E. T. Penny 1993 *Modal Analysis*: *The International Journal of Analytical and Experimental Modal Analysis* **8**, 257–262. The choice of orthogonal polynomials in the rational fraction polynomial method.
28. D. M. Smith 1969 *Journal Bearings in Turbomachinery*. London: Chapman and Hall.